

N90-29840

Performance Limitations of Bilateral Force Reflection Imposed by Operator Dynamic Characteristics

Jim D. Chapel

Martin Marietta Astronautics Group
Denver, Colorado

Abstract

This paper presents a linearized, single-axis model for bilateral force reflection which facilitates investigation into the effects of manipulator, operator, and task dynamics, as well as time delay and gain scaling. Structural similarities are noted between this model and impedance control. Stability results based upon this model impose requirements upon operator dynamic characteristics as functions of system time delay and environmental stiffness. An experimental characterization reveals the limited capabilities of the human operator to meet these requirements. A procedure is presented for determining the force reflection gain scaling required to provide stability and acceptable operator workload. This procedure is applied to a system with dynamics typical of a space manipulator, and the required gain scaling is presented as a function of environmental stiffness.

1. Introduction

The development of NASA's Flight Telerobotic Servicer (FTS) provides the robotics research community many engineering challenges which must be addressed to provide a safe and effective space-based teleoperation system. One of the problems confronting this new initiative is the adaptation of control techniques widely used in nuclear and undersea teleoperation systems to a space-based system. The control techniques utilized in these existing systems have evolved over the past three decades to provide the operator with an interface that is comfortable and nearly transparent. However, the teleoperation technology base developed during this time period is not broad enough to facilitate engineering design and performance prediction for a system with significantly different characteristics. Digital sampling and communication delay inherent in a space teleoperation system have been shown to degrade the performance and stability of force-reflecting teleoperation systems [1,2]. Additionally, the dynamics of manipulators designed for use in space, as shown in Figure 1, are likely to be significantly different from those of manipulators designed for terrestrial applications. To facilitate a rational design process, a model-based analysis is needed that can predict performance of teleoperation control schemes when implemented in any specific system.

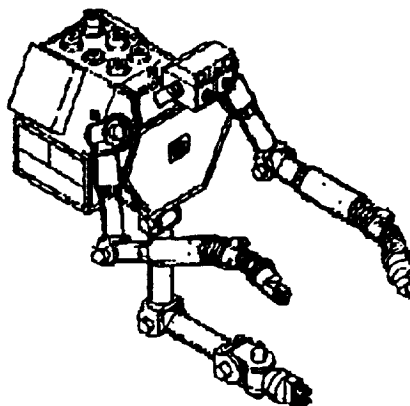


Figure 1 Early Flight Telerobotic Servicer Concept

This paper examines the dynamic characteristics of force-reflecting teleoperation systems, and investigates the effects of communication time delay, digital sampling, task dynamics, and operator dynamics on stability and performance. The technical approach presented here examines the dynamic characteristics of bilateral force reflection by exploiting similarities between bilateral force reflection and position-based impedance control. In both cases, a dynamic relationship is established between the measured environmental force and commanded manipulator position. In the case of impedance control, this relationship is realized by specifying parameters in a digital "impedance" filter, whereas in the case of bilateral force reflection, this relationship is determined by the dynamic characteristics of the human operator/hand controller combination. Unlike the impedance filter parameters, the human operator dynamic characteristics are nonlinear and time varying. Analysis of the linear time invariant problem generates stability boundaries for impedance filter design as functions of communication time delay, digital sampling and task dynamics [1,3,4]. Comparison of the impedance filter parameters to the physical parameters of the human operator/hand controller model reveals that this stability analysis imposes requirements on human operator stiffness and damping.

An experimental frequency response characterization of five test subjects is presented that quantifies the limited capabilities of human operators to provide the dynamic parameters needed to stabilize the system. The dominant features in the frequency range of interest are found to be captured using a second order model parameterized by stiffness, damping, and inertia. Test results are presented for minimum, moderate, and maximum exertion levels. Operator dynamic parameters are demonstrated to be closely coupled over the range of capability, i.e., operator stiffness cannot be generated independent of operator damping. The results of this characterization provide a basis for determining operational capabilities and limitations of force-reflecting teleoperation systems controlled by human operators.

The impedance control stability analysis imposes requirements on dynamic compensation in the force reflection loop, and the operator dynamic characterization provides the limits of human capabilities to provide this compensation. Comparison of human operator capabilities to the dynamic feedback requirements can be used to determine the stability and operator workload of bilateral force reflection. If the system is not stable, or the resulting workload is considered excessive, the analysis presented also shows how gains within the system, namely the force reflection and position gains, can be adjusted to provide acceptable performance.

2. Teleoperator Force Reflection Analysis

The free-space position response of the teleoperation system's manipulator is assumed to be accurately modeled by a second order transfer function. This assumption is valid for position controlled manipulators that do not exhibit flexible modes in the frequency range of interest, which is generally less than 10 Hz. Although the coefficients of this transfer function vary depending upon the manipulator's pose, the following analysis considers operation about a point in space so that the transfer function coefficients can be assumed constant. Stiffness is often the dominant effect of the environment, especially for assembly and maintenance tasks using metal parts. The environment can then be modeled by a single stiffness term, K_e . The transfer function relating position response to position command for the manipulator in contact with the environment is then given by

$$\frac{X}{X_c} = \frac{K_m}{J_m s^2 + B_m s + K_m + K_e} \quad (1)$$

where K_m , B_m , J_m are the controlled manipulator stiffness, damping, and inertia, respectively. The forces seen at the manipulator are assumed reflected back to the hand controller through a

communication link with time delay $T_d/2$. A feedback gain, K_f , is provided to scale the sensed environmental forces to a comfortable level for the operator. The human operator/hand controller system can be modeled as a second order dynamic system as well, but the transfer function coefficients are not constant because of varying levels of operator exertion. For this analysis, the operator dynamic parameters are assumed constant during the environmental interaction being studied. The resulting transfer function relating reflected force to hand controller position is given by

$$\frac{X_{hc}}{F} = \frac{1}{Js^2 + Bs + K} \quad (2)$$

where K , B , and J are the stiffness, damping, and inertia of the human operator/hand controller combination, respectively. A feedforward gain, K_p , is also provided to scale the hand controller motion to commanded manipulator motion. Finally, the commanded manipulator position is issued to the manipulator through a communication link with time delay $T_d/2$. The open loop transfer function of the system is given by

$$T(s) = \frac{K_p K_f K_e K_m e^{-sT_d}}{(J_m s^2 + B_m s + K_m + K_e)(Js^2 + Bs + K)} \quad (3)$$

Figure 2 presents the system structure in block diagram form. A reference input is introduced as representative of the operator inputs to the hand controller. Examining the block diagram of this system, we can see that bilateral force reflection forms a feedback control scheme with a dynamic compensator. The dynamics of the manipulator, the environment, and the operator/hand controller combination, as well as communication/computation time delay and control law gains, are all important in determining the stability of bilateral force reflection. Studying the magnitude and phase characteristics of the open loop transfer function given in Eq. (3) provides insight into the stability and performance of force-reflecting teleoperation systems that can be modeled as shown in Figure 2.

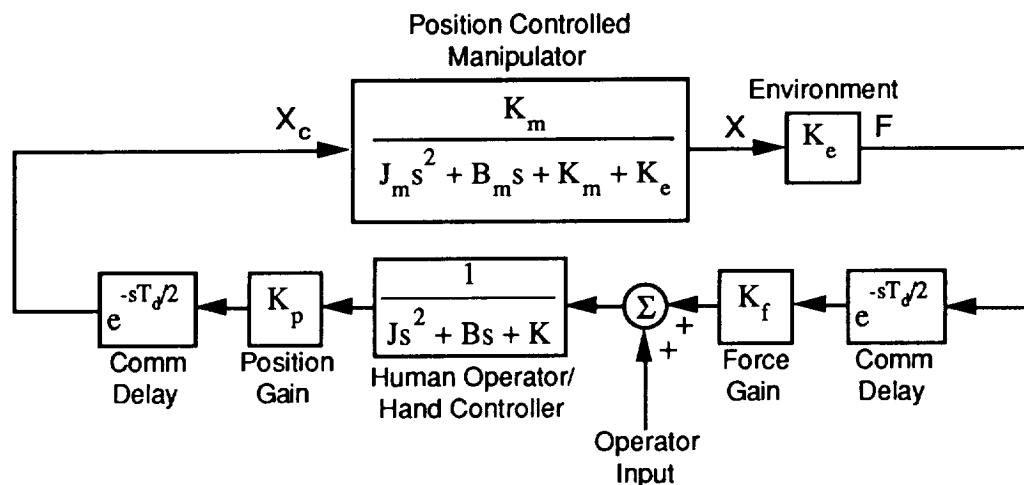


Figure 2 Force-Reflecting Teleoperation Block Diagram

When the structure of this form of force reflection is compared to those of other forms of active force control, it is seen that the structure presented here is identical to the "impedance control" structure described in the robotic systems literature [5,6]. In both cases, the position command issued to the

manipulator is modified by sensed environmental forces passed through a dynamic filter, thereby establishing a dynamic relationship between manipulator force and position. This relationship can be interpreted as a mechanical "impedance." Unlike the impedance control case where impedance filter parameters can be programmed arbitrarily, bilateral force reflection has a limited capability of providing filter parameters because of the human operator's physical limitations. Even so, the requirements on the physical dynamics of the human operator/hand controller are identical to those imposed on the impedance filter dynamics to ensure stability. This allows stability analysis results derived for impedance control to be applied to this problem. Details of the analysis have been previously published [3,4], and will not be repeated here. A summary of the approach and the results of this analysis are presented in the following discussion.

To find the stability boundaries of an impedance control system with a second order impedance filter described by Eq. (2), the parameters must be found for the open-loop transfer function in Eq. (3) that result in a marginally stable system. Because we are interested in impedance filter design requirements, we wish to find the parameters J , B , and K that produce a marginally stable system while the other parameters in the system remain fixed. If the characteristic equations of both the manipulator and impedance filter transfer functions in Eqs. (1) and (2) have damping ratios of at least 0.707, the magnitude response is a monotone decreasing function of frequency. This requirement implies that no resonant peaks be present in the magnitude response for either of these parts of the system. If the impedance filter represents the human operator/hand controller dynamics, this would normally be the case to provide acceptable performance and feel. The manipulator control system would typically be designed to exhibit this characteristic when not in contact with the environment, but the damping ratio of the characteristic equation of Eq. (2) decreases as the environmental stiffness, K_e , increases. For some range of environmental stiffnesses, the damping ratio of the manipulator's position response would still be greater than 0.707. The case where this assumption is not valid is discussed later in this paper. If the damping assumption holds, the simultaneous solution of the magnitude equation for a magnitude of unity and the phase equation for a phase angle of -180 degrees provides a unique solution for the impedance filter parameter K given J and B . Introduction of time delay into the system decreases the phase linearly with frequency and therefore does not affect the uniqueness of solution.

Numerically solving this nonlinear system of equations with various communication/computation time delays, we find stability boundaries on the K - B plane of the form shown in Figure 3. For the solution shown, the impedance filter parameter corresponding to the hand controller inertia, J , was set to zero. This assumption is equivalent to the inertia of the operator/hand controller combination being small compared with its stiffness and damping characteristics. Manipulator parameters used for the stability boundaries presented in Figure 3 are representative of dextrous space manipulators, corresponding to a manipulator weighing 150 lbs being controlled by a moderate performance position controller with a bandwidth of 1.5 Hz. Experimental studies using an impedance-controlled industrial manipulator have verified the general characteristics of these stability boundaries, and have also shown close agreement between analytical predictions and experimental measurements [3].

Interpreting the results shown in Figure 3 for the case of force-reflecting teleoperation, we see that the stiffness and damping that must be provided by the operator are quantified for the system with the given parameters. It is important to note that even with no time delay in the system, some operator stiffness and damping is required to stabilize the system. This phenomenon is caused by the phase lag or transport delay of the position-controlled manipulator. Not surprisingly, increasing the time delay within the system while keeping the control gains the same increases the requirements for operator stiffness and/or damping to retain stability. Because the operator provides stiffness and damping to the system by tightening his arm muscles, increased time delay sharply increases the physical workload of the operator. Additionally, the increased requirements may exceed the operator's capability to stabilize the system. Because the stiffness and damping parameters required are the ratios of operator stiffness and damping to the product of the control gains, decreasing the position gain, K_p , the force reflection gain, K_f , or both reduces the stiffness and damping

requirements of the operator. In this way, a system with arbitrarily large time delay can be stabilized. Although it is certainly possible to decrease the force reflection gain to have a stable system with several seconds of time delay, the gain would be so small that force reflection would be effectively disabled. Smaller reductions in the control gains also degrade the performance of force reflection by reducing the "crispness" or "feel" of the system.

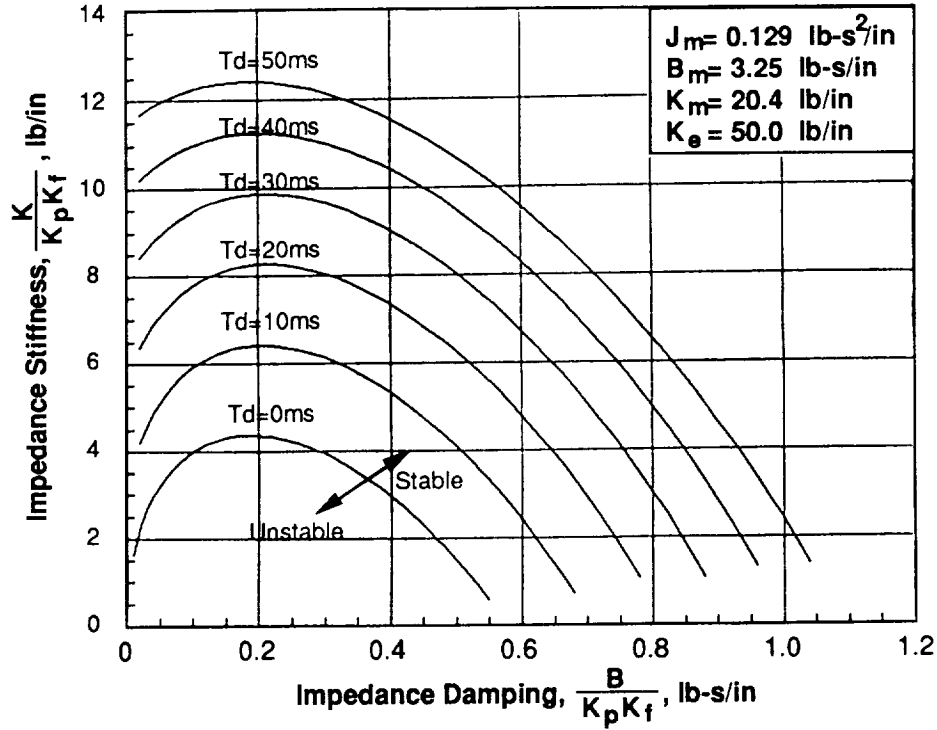


Figure 3 Stability Boundaries as a Function of Time Delay

Families of solutions can also be generated on the K-B plane for different values of the environmental stiffness. For systems with no time delays, the Routh-Hurwitz criterion can be used to determine stability conditions on K, B, and J [3]. If K and B are restricted to being positive real numbers and J is again set to zero, the constraint equation for K and B to retain stability is given by

$$K > -B \frac{B_m}{2J_m} + \sqrt{B^2 \left(\frac{B_m^2}{4J_m^2} - \frac{K_e + K_m}{J_m} \right) + B \frac{K_p K_f K_e K_m}{B_m}} \quad (4)$$

If the controlled manipulator dynamic characteristics, J_m , B_m and K_m , are held constant and K_e is allowed to vary, the relationship in Eq. (4) produces a family of stability boundaries parameterized by B, K, and K_e . Using the same manipulator dynamics that were used to generate the plot in Figure 3, we can find these stability boundaries in the K-B plane as shown in Figure 4. For a given set of control gains, larger environmental stiffnesses require higher values of stiffness and damping from the operator. Higher environmental stiffnesses therefore require higher operator workload and will generally produce a less stable system. As discussed before, the control gains K_p and K_f can be adjusted to guarantee that the system is stable, but at the cost of making the environment feel more spongy to the operator.

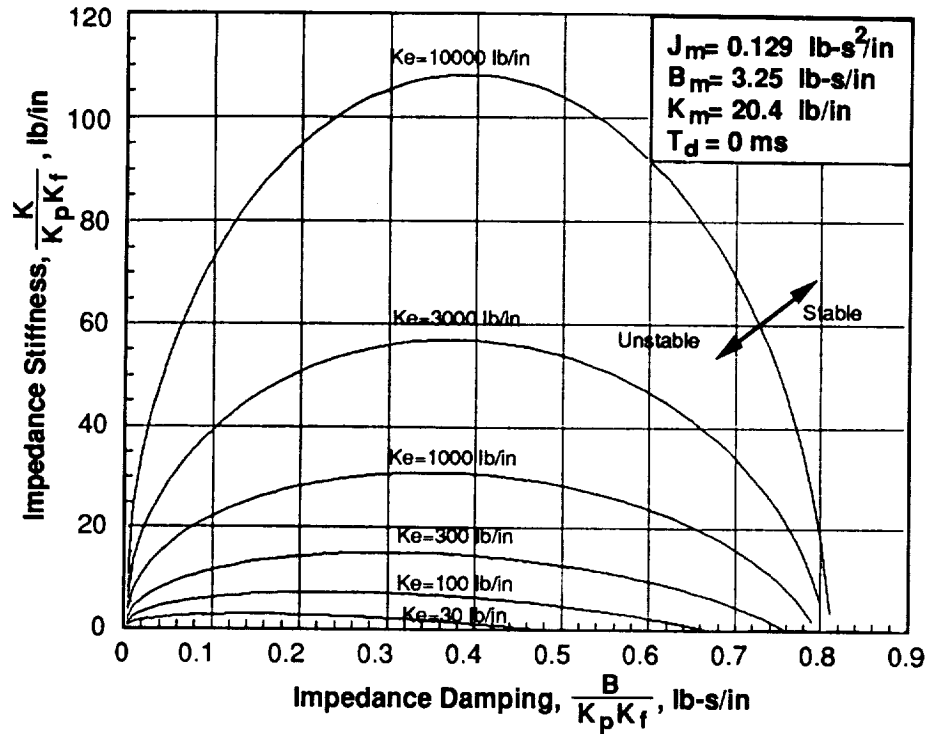


Figure 4 Stability Boundaries as a Function of Environmental Stiffness

If time delay is introduced in to the system, an analytical solution can no longer be obtained. As long as the environmental stiffness, K_e , is not large enough to produce a resonant peak in the magnitude response of Eq. (1), the same method of solution can be used to find stability boundaries for various environmental stiffnesses as was used to find the stability boundaries for various time delays. When a resonant peak is present in the magnitude response of the manipulator transfer function, the simultaneous solution of the magnitude and phase equations for a magnitude of unity and phase of -180 degrees no longer guarantees a marginally stable system. To find the values of K , B and J that produce a marginally stable system in this case, the Nyquist plot needs to be found that crosses the real axis at the -1 point and does not encircle the -1 point. Because the resonant mode produces a nearly circular contour in the Nyquist plane [7] and the phase changes rapidly near the resonant frequency, the real-axis intersection is approximately given by the real part of the open-loop transfer function, $T(s)$, evaluated at the resonant frequency. Use of this approximation results in the following stability constraint:

$$\text{Re} (T(j\omega_r)) > -1 \quad (5)$$

where ω_r is the resonant frequency of Eq. 1. This approximation is most accurate when the damping of the manipulator dynamics is small, or alternatively, when the environmental stiffness is large. The dynamics of the manipulator in contact with the environment are already known, so this constraint imposes limits on the impedance filter to maintain stability. The constraint given in Eq. (5) can then be used to determine the constraints upon impedance filter design to stabilize systems with time delay.

3. Human Operator Dynamic Characterization

The stability analysis presented above provides requirements for any dynamic force compensation implemented in the structure of Figure 1. Force-reflecting teleoperation is of this form and therefore requires specific human operator dynamic characteristics to retain stability. An experiment is presented here that determines operator dynamic characteristics over a range of test subjects from minimum to maximum exertion levels. Comparison of the experimentally demonstrated capabilities to the requirements derived from the stability analysis provides information about system stability and operator workload.

To investigate the operator dynamic characteristics, a one-DOF hand controller was set up as shown in Figure 5. The test setup consisted of an Inland brush motor attached to the input shaft of a harmonic drive with a 100:1 gear ratio. To obtain primarily translation motion, a hand grip with a 12 inch link was attached to the output shaft of the harmonic drive. The effects of drive friction and reflected inertia were minimized by implementing a moderate bandwidth analog torque loop on the harmonic drive. A conductive plastic potentiometer, mounted on the motor shaft, was used as the angular position sensor. The resulting one-DOF hand controller had the desirable characteristic of high torque levels yet was still responsive to extremely small operator force inputs.

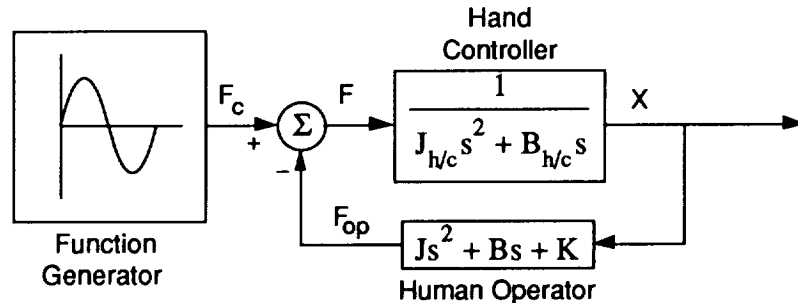


Figure 5 One-DOF Hand Controller Testbed

A set of five operators was tested using this experimental hand controller configuration. Motion in the direction forward from the body was chosen as representative of many teleoperation assembly and insertion tasks. Frequency response data was taken from 1.0 Hz to 6.0 Hz to obtain the transfer function between hand controller force and position. Each operator made three runs consisting of minimum operator exertion, moderate operator exertion, and maximum operator exertion. The torque input was set such that the operators could not stop hand controller motion even when exerting maximum force. Stiffness, damping, and inertia parameters were extracted from the frequency response data by first fitting a second order response to the frequency response data. The dc level was used to extract the operator stiffness, K. The second order curve fit and the parameter K were then used to determine the operator damping and inertia, B and J, respectively. These parameters represent the dynamics of the human operator/hand controller combination in Eq. (2). By subtracting off the hand controller damping and inertia terms, $B_{h/c}$ and $J_{h/c}$, determined from a separate open-loop frequency response on the hand controller alone, the human operator dynamic parameters can be determined.

The stiffness and damping characteristics of the human operators, determined by the method described above, are shown in Figure 6. For each operator, effective inertia displayed only a small variation between runs compared with the variation in the stiffness and damping parameters. The maximum inertia values were observed for the maximum exertion case where the operators attempted to resist hand controller motion by tensing the upper body muscles. Because more body mass is active during hand controller motion in this case, an increase in effective operator inertia of

approximately a factor of two was observed for each operator. Measured operator inertias displayed negligible variation between minimum and moderate exertion runs.

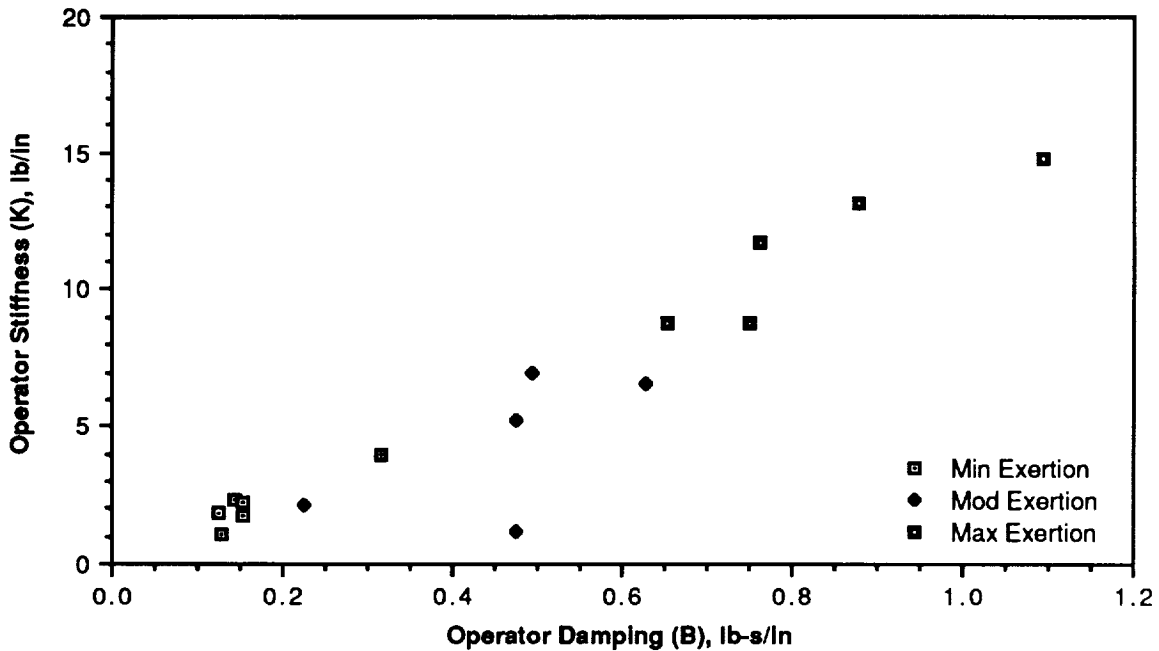


Figure 6 Operator Characterization Results

Two key results are observed from this testing. First, human operators clearly have limited capabilities for providing stiffness and damping to stabilize force-reflecting teleoperation systems. In the direction forward from the body, system designs requiring more than 10 lb/in stiffness or more than 0.7 lb-s/in damping would be unacceptable for prolonged operation. Systems requiring more than 15 lb/in stiffness or more than 1.1 lb-s/in damping could not be stabilized by human operators in this direction. Second, stiffness and damping apparently cannot be provided independently by human operators. In fact, the two parameters appear to be linearly related. This simplifies the required stability analysis because only a small range of the stability boundaries need to be examined to determine stability of the overall system and operator workload.

4. Teleoperation Performance and Stability Implications

The results of the stability analysis can be combined with the human operator characterization data to predict whether or not a force-reflecting teleoperation system can be stabilized by a human operator. If the operator is able to provide the required stiffness and damping characteristics, the operator workload can be predicted by examining the location of the required dynamic characteristics within the range of operator capabilities. Finally, if the system cannot be stabilized by the operator, or the workload is considered unacceptable, the required force reflection gain, K_f , and position gain, K_p , can be computed to ensure system stability and appropriate workload level. Examining the same system presented in the stability analysis above and considering the case where there is no time delay in the system, we can determine system stability, operator workload, and required gain scaling for the ideal situation. As shown in Figure 3, the addition of time delay into the system will increase operator dynamic requirements or, alternatively, will increase gain scaling requirements.

To compare the requirements of the force reflection compensator with the capabilities of the human operator for this ideal case, a linear curvefit is first made to the data shown in Figure 6. This linear equation is then scaled by K_p and K_f to account for non-unity control gains, and the resulting equation modeling the human operator can be written as

$$\frac{K}{K_p K_f} = 14.2 \frac{B}{K_p K_f} \quad (6)$$

Overplotting Eq. (6) on Figure 4 provides a comparison between the human operator dynamic characteristics and the stability behavior of the force-reflecting system given in Figure 2 as the environmental stiffness is allowed to vary. By searching along the line given by Eq. (6), we can find environmental stiffness values that produce a marginally stable system for particular values of $K/K_p K_f$ and $B/K_p K_f$. However, the human operator has clear limitations on providing stiffness, K , and damping, B . If the operational limitations of the operator are used for K and B in Eq. (6), the gain scaling required to provide a marginally stable system can be found as a function of the environmental stiffness. Examination of the data from Figure 6 shows that an operator stiffness of less than 8 lb/in was easily provided by the operators. Stiffness values above 10 lb/in required an excessive amount of effort and would not normally be considered as within the operators' capability range. Stiffness values between 8 lb/in and 10 lb/in required substantial effort but could be provided comfortably for short periods of time. Operator stiffness values of 8 lb/in and 10 lb/in, along with the corresponding operator damping values from Eq. (6), were used to find the required control gain, $K_p K_f$, to provide a marginally stable system as a function of the environmental stiffness, K_e . The resulting plot of $K_p K_f$ as a function of K_e is shown in Figure 7.

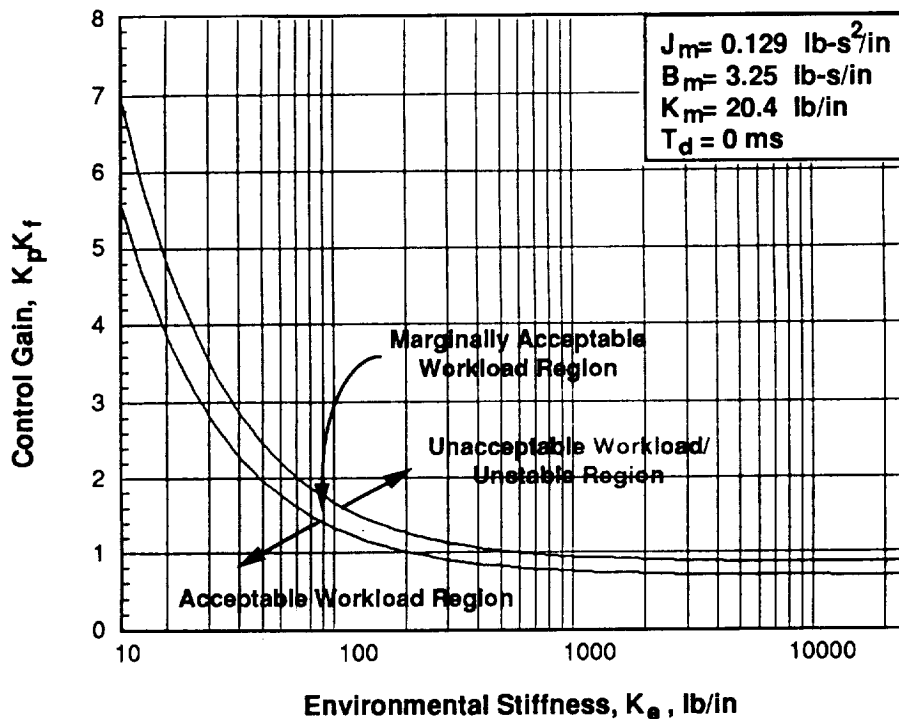


Figure 7 Gain Scaling Required to Stabilize Force Reflection

Examining the curves shown in Figure 7, we see that the product of the control gains, $K_p K_f$, can be greater than unity for small environmental stiffnesses. The allowable control gains decrease with increasing environmental stiffness. Even with no time delay, this system cannot be stabilized by the operator when the product of the control gains, $K_p K_f$, is unity and K_e is greater than 500 lb/in. Either the position gain, K_p , or the force reflection gain, K_f , or both must be reduced to operate this system in contact with stiff environments. The $K_p K_f$ curve becomes flat as K_e increases above 1000 lb/in. Because of this, a single value of $K_p K_f$ can be used for a large range of stiff environments.

5. Summary

The existing teleoperation technology base needs to be expanded to allow efficient design, development and deployment of the first generation of dexterous space robots. The initial work presented here has examined the stability and performance of the bilateral force reflection control scheme, commonly used in current teleoperation systems, when incorporated into a system with characteristics typical of space manipulators. Because of the similarities between this control scheme and the active force control scheme known as "impedance control," recent stability results from the analysis of impedance control can be applied to this system. These analyses show that time delays as small as 10 ms, such as those caused by communication delay or computation time, can significantly increase the stiffness and damping required from the operator to stabilize the system. The stiffness of the environment is also important in determining the stability of the system. Interaction with stiff work pieces requires large operator stiffness and damping parameters to retain stability. Experimental data has shown the operator stiffness and damping characteristics to be tightly coupled, and has shown the maximum operational values for operator stiffness and damping to be 10 lb/in and 0.7 lb-s/in, respectively, for the translational direction forward from the body. Scaling of the position and/or force control gains will allow any system to be stabilized, but at the cost of reducing the feel to the operator. A procedure was introduced that uses the operator model to find the required gain scaling as a function of the environmental stiffness. Even with no time delay, the example system representative of a space manipulator would require gain scaling when interacting with environmental stiffnesses larger than 500 lb/in. However, a large range of high stiffness values can be accommodated with little or no change in the gain scaling. Analysis of time delay effects indicates that more gain scaling would be required for a model including time delay. The further development of the understanding of how these critical system parameters affect overall stability and performance will allow standard engineering design techniques to be used to develop an effective control strategy for any specific telerobot system.

6. References

1. Chapel, J. D., and Lawrence, D. A., "Stability Analysis for Alternative Force Control Schemes as Applied to Remote Space Teleoperation," Proceedings of the 10th Annual AAS Guidance and Control Conference, February 1987.
2. Hannaford, B., and Anderson, A., "Experimental and Simulation Studies of Hard Contact in Force Reflecting Teleoperation," Proceedings of the 1988 IEEE International Conference on Robotics and Automation, April 1988.
3. Lawrence, D. A., and Stoughton, R. M., "Position-Based Impedance Control: Achieving Stability in Practice," Proceedings of the 1987 AIAA Guidance, Navigation, and Control Conference, August 1987.
4. Lawrence, D. A., "Impedance Control Stability Properties in Common Implementations," Proceedings of the 1988 IEEE International Conference on Robotics and Automation, April 1988.
5. Whitney, D. E., "Force Feedback Control of Manipulator Fine Motions," ASME Journal of Dynamic Systems, Measurement, and Control, June 1977, pp. 91-97.
6. Hogan, N., "Impedance Control: An Approach to Manipulation," ASME Journal of Dynamic Systems, Measurement, and Control, March 1985, pp. 1-24.
7. Ewins, D. J., Modal Testing: Theory and Practice, Research Studies Press Ltd, Letchworth England, 1984, pp. 158-168.